Applied Clay Science 258 (2024) 107451

Contents lists available at ScienceDirect

Applied Clay Science

journal homepage: www.elsevier.com/locate/clay

Research Paper

A recycled natural resource as secondary raw material for versatile technological applications: the quarry waste from zeolite-rich tuffs

Sossio Fabio Graziano [a,*], Mariano Mercurio [b], Francesco Izzo [c], Alessio Langella [c], Concetta Rispoli [c], Nicola Davide Santaniello [c], Claudia Di Benedetto [c], Vincenzo Monetti [c], Marco Biondi [a], Giuseppe De Rosa [a], Laura Mayol [d], Fabrizio Villapiano [a], Michele Dondi [e], Chiara Zanelli [e], Chiara Molinari [e], Barbara Liguori [f], Assunta Campanile [f], Piergiulio Cappelletti [c,g]

[a] Department of Pharmacy, Federico II University, Via Domenico Montesano, 49, 80131 Napoli, Italy
[b] Department of Science and Technology, University of Sannio, Via dei Mulini, 42, 82100 Benevento, Italy
[c] Department of Earth Sciences, Environment and Resources, Federico II University, Via Vicinale Cupa Cintia, 21, 80126 Napoli, Italy
[d] Department of Advanced Biomedical Sciences, Federico II University, Via Pansini 5, 80131 Napoli, Italy
[e] CNR-ISTEC, via Granarolo 64, 48018 Faenza, Italy
[f] Department of Chemical Engineering, Materials and Industrial Production, Federico II University, Piazzale Vincenzo Tecchio, 80, 80125 Napoli, Italy
[g] Centro Musei delle Scienze Naturali e Fisiche, Federico II University, Via Mezzocannone, 8, 80134 Napoli, Italy

ARTICLE INFO

Keywords:
Zeolite rich tuffs
Sorano Formation
Quarry waste
Lightweight expanded aggregates
Pozzolanic activity
Drug carrier

ABSTRACT

Natural resources, along with critical raw materials, are increasingly considered a focus for technological applications. Widely available and inexpensive natural resources, such as zeolite-rich geomaterials, possess minerochemical characteristics that make them very useful in various technological applications, representing a strategic choice with a strong green connotation. In this research, the possibility of recycling waste powders from quarrying operations of zeolite-rich tuffs in technological applications for the construction sector and drug delivery was investigated.

Waste powders collected from quarries operating on the Sorano Formation (Tuscany - Italy), were used for a preliminary characterization, performed to evaluate zeolite content and potential pollution deriving from industrial processing.

Thereafter, the specific technological characterization was carried out to define the waste attitude to represent a promising candidate raw material for Lightweight Expanded Aggregates (LEA) production, partial substitution component with pozzolanic activity in cement formulations, carrier for active pharmaceutical molecules.

Experimental results, obtained following European normative, proved that was possible to produce waste-based LEA with comparable features with those reported for currently marketed products, that waste powders exhibited pozzolanic activity evidencing the possible use as addition for blended cements and, finally, the use of a cationic surfactant determined a surface-modification of natural zeolites (contained in waste samples) which encouraged for an early loading trial of active pharmaceutical molecules.

This research can be safely extended to other quarry waste, with similar mineralogical and chemical composition, leading to a strong contribution in the waste management of this sector.

1. Introduction

Natural resources are increasingly being used for technological applications to improve industrial and civil technological processes.

Along with the concern on critical and strategic raw materials (Girtan et al., 2021; European Commission, 2023), there is a growing focus on upgrading resources that are widely available and inexpensive but reveal surprising and versatile technological characteristics. These include natural zeolites, which applications range from established utilization, e.g. in agriculture and animal feed (Papaioannou et al.,

* Corresponding author.
E-mail address: sgraziano@unina.it (S.F. Graziano).

https://doi.org/10.1016/j.clay.2024.107451
Received 15 February 2024; Received in revised form 3 June 2024; Accepted 5 June 2024
Available online 14 June 2024
0169-1317/© 2024 The Author(s). Published by Elsevier B.V. This is an open access article under the CC BY-NC-ND license (http://creativecommons.org/licenses/by-nc-nd/4.0/).

2005; Eroglu et al., 2017) to potential uses with high added value, such as pharmaceuticals, environmental remediation, etc. (Cappelletti et al., 2017; König et al., 2020; Serati-Nouri et al., 2020; Morante-Carballo et al., 2021) which have yet to be brought to a level of technological readiness suitable for market demands.

The recent literature offers several examples of novel solutions to improve materials and technologies by natural zeolites: drug delivery (Servatan et al., 2020) catalysis and chemical processes (Jin et al., 2024; Liu and Zhu, 2024); selective adsorption of toxic compounds from waste water and the environment (Bogusz et al., 2024; Ismail et al., 2024; Liu et al., 2024; Öz, 2024; Zhou et al., 2024); skin protection and health care (Fantini et al., 2024); carbon capture (Selim et al., 2024); innovative and eco-designed building materials (Vaičiukynienė et al., 2024; Wei et al., 2024; Yudi et al., 2024; Zhu et al., 2024).

These opportunities involve raw materials that are not pure zeolites, strictly speaking, but more or less extensively zeolitized rocks, where the zeolitic component is usually predominant but other phases (crystalline and non-crystalline) may be present (Giampaolo et al., 2008; Langella et al., 2013; Gentili et al., 2014; Belkin et al., 2016; Mormone et al., 2018; Rolandi et al., 2019a, 2019b). For this reason, it is essential to know in detail the genetic processes that lead to the formation of the phases of interest, in order to better understand the variations in the zeolite content of the deposit and, consequently, variations in the technological properties of the materials that will be used (Giampaolo et al., 2008; Bear et al., 2009; Fercia et al., 2009; Langella et al., 2013, 2022; Bareschino et al., 2017, 2019; Skhvitaridze et al., 2018; Izzo et al., 2022).

These resources are, from the point of view of economic geology, between well-characterized and widely exploited zeolite deposits (Holmes, 1994; St. Cloud Mining Co., 2024) and others with a great potential, but underexploited and little known scientifically (de Gennaro et al., 2007, 2009; Cappelletti et al., 2011; Graziano et al., 2016; Izzo et al., 2022). The challenge is to valorize these natural deposits by developing technological solutions that enable the use in applications of greater value, although not as demanding as in the case of synthetic zeolites. Zeolite-rich deposits that have been exploiting since decades can represent a tested to verify how to widen the possible uses towards applications with greater added value (Gualtieri et al., 1999; Vereshchagin and Sokolova, 2006; de Gennaro et al., 2008; Pasquino et al., 2016; Bareschino et al., 2017; Cappelletti et al., 2017; Krajišnik et al., 2018; Liguori et al., 2019; Serati-Nouri et al., 2020; Smiljanić et al., 2020; Cataldo et al., 2021; Morante-Carballo et al., 2021; Moreno Ríos et al., 2022; Noviello et al., 2021; Takarina et al., 2024; Taoufik et al., 2020). A specific target is the widely available quarry dust from cutting and processing these geomaterials for building purposes, thus transforming a waste into an added value by-product. This waste material is currently employed in animal farming (dietary supplement, pet litter and manure deodorizer) as well as in agriculture as soil amendant and slow-release fertilizers (Biesek et al., 2021; Brumovská et al., 2021; Cataldo et al., 2021; El-Nile et al., 2021; Herc et al., 2021; Holanda et al., 2021; Noviello et al., 2021; Wang et al., 2021; Banaszak et al., 2022; Feoktistova et al., 2022; Ghoneem et al., 2022; Javed et al., 2022; Vafaee and Chaji, 2022; Kumar et al., 2023; Pavlak et al., 2023; Rashid and Rafey, 2023).

The Quaternary volcanism of the central-southern Italy can be a suitable case-study, as it emplaced huge volcaniclastic and pyroclastic deposits, often deeply affected by intense sin- and post-depositional minerogenetic processes leading to the transformation of reactive volcanic glass in zeolites, with subsequent lithification of the deposits (de' Gennaro et al., 2000; Cappelletti et al., 2003, 2015; Langella et al., 2013; Colella et al., 2017; Novembre et al., 2021; Peccerillo, 2017). The main use has been as dimension stones in the building industry, by exploiting their low cost, volume weight, mechanical features, and the excellent thermal insulation (de' Gennaro and Langella, 1996). These natural zeolites (sometimes occurring in the rock up to 70-80 wt%) have been studied, based on the good cation exchange capacity and adsorption properties, for various applications (Carbonchi et al., 1999; de Gennaro et al., 2004, 2005, 2007, 2008, 2009; Monteiro et al., 2004, 2005; Cappelletti et al., 2011, 2017; Liguori et al., 2015, 2019; Dondi et al., 2016; Özen et al., 2016; Pasquino et al., 2016; Serri et al., 2016; Mercurio et al., 2018, 2019; Izzo et al., 2019; Smiljanić et al., 2020, 2021; Montesano et al., 2022).

In this paper, a pyroclastic deposit from the Latera volcano (Vulsini Volcanic District, VVD, central Italy) pertaining to the Sorano Formation, was considered for sampling (Vezzoli et al., 1987; Palladino and Simei, 2005; Valentine et al., 2019, Washington, 1906 - Appendix, fig. A1).

From a petrographic point of view, this lithoid yellow tuff, also described as D-Ignimbrite, is a very fine-grained trachytic deposit as thick as tens of meters with a glass composition (the precursor of the zeolites) varying from trachybasalt and phonotephrite to trachyte and phonolite (Sparks, 1975; Landi, 1987; Nappi et al., 1987, 1998; Vezzoli et al., 1987; Turbeville, 1992; Conticelli et al., 1997; Renzulli et al., 2018). In addition, the deposits were deeply affected by intense secondary mineralogical processes, leading to the crystallization of zeolites, mainly represented by chabazite (subordinate phillipsite) through the transformation of primary volcanic glasses (Cappelletti et al., 1999).

Waste material from two mining sites was then subjected to minero-petrographical characterization and then technological testing. Along with about 23,000 tons/year of finished product, approximately 9000 tons/year of waste is produced (i.e., 40% of the deposit, without waste recycling, is landfilled).

The possibility of reusing these quarry wastes, containing zeolites in good quantities, as raw material for technological applications was tested for potential applications in the production of lightweight expanded aggregate (LEA), as a pozzolanic additive in cement production, and as a carrier of pharmacologically active molecules.

2. Material and methods

This research is focused on investigating materials sampled from two active quarries: C quarry (42°40'41.27" N; 11°42'01.15" E) and P quarry (42°41'25.52" N; 11°44'38.29" E), both operating on zeolite-rich tuffs from the Sorano Formation (Geological service - Tuscany region. Italy, 2013).

Since identified quarries are mainly devoted to produce dimension stones, both samples of building stones and waste powders, were collected and identified as follows:

- C1 and P1 – Quarry finished products – building material produced by quarry operations (respectively C and P quarry).
- C2 and P2 - Powdered sample – waste from quarry operations (respectively C and P quarry).

2.1. Mineralogical composition

Mineralogical qualitative and quantitative analyses were carried out by means of X-ray powder diffraction (XRPD) using a Panalytical X'Pert Pro diffractometer, equipped with a RTMS X'Celerator detector with monochromed Cu-Kα radiation, operating at 40 kV and 40 mA. Sample powders were mill-micronized (<10 μm particle size) by using a Retsch XRD-Mill McCrone and added with a 20% Buelher α-alumina for quantitative reference and then prepared on the related sample holders avoiding isoorientation or non-flat surface. Collecting conditions for scans were: range 5–70°2θ with a step interval of 0.017°2θ and a time per step of 120 s. Mineral phases were identified by the Panalytical Highscore Plus 3.0e software and PDF-2/ICSD mineral databases. Quantitative analyses were performed by Reference Intensity Ratio – full profile (RIR-Rietveld) combined methods (Bish and Howard, 1988; Bish and Post, 1993; Rietveld, 1969) using Topas software (version 5.0, Bruker, Germany).

2.2. Chemical composition

Chemical analyses were performed using an Axios Panalytical X-ray fluorescence (XRF) spectrometer, equipped with six analyzer crystals, three primary collimators and two detectors.

Sample powders were mixed with polyvinyl alcohol and prepared in aluminum cups with the bottom first filled with boric acid, to be sure that infinite thickness was achieved; the aluminum cup was then compacted with a hydraulic press to obtain flat surface discs.

Analytical percentage uncertainties are 1–2% relative (Cucciniello et al., 2017). The weight Loss on Ignition (L.o.I.), determined by gravimetric techniques, was evaluated by firing at 1000 °C for 2 h sample powders previously dried at 110 °C overnight (ASTM International, 2021).

2.3. Scanning Electron Microscopy – Energy Dispersive Spectrometer microanalyses

Microstructural investigations were performed by means of a Field Emission Scanning Electron Microscope equipped with an Energy Dispersive Spectrometer (FESEM/EDS; Zeiss Merlin VP Compact coupled with Oxford Instruments Microanalysis Unit; Carl-Zeiss- Strasse, Oberkochen, Germany) both used for observations and spot analyses. Data sets were obtained using an INCA X-stream pulse processor (Oberkochen, Germany) (15-*k*V primary beam voltage, 50–100 A filament current, variable spot size, from 30,000 to 200,000× magnification, 20 mm working distance, and 50 s real-time counting) by means of INCA Energy software 5.05 (XPP array and pulse pile-up corrections).

2.4. Mercury Intrusion Porosimetry

Mercury Intrusion Porosimetry (MIP) tests were performed using a Thermo Finnigan Pascal Hg porosimeter with 140 and 440 devices. The first one applies a low mercury pressure up to 400 kPa to introduce mercury into the sample and to measure the macroporosity. The second one applies a maximum pressure of 400 MPa for the measurement of meso-porosity (pore radius ranging from 58 to 0.0019 μm (Rouquerol et al., 1994; IUPAC ISO 15901-1-2005, 2005).

Small but representative fragments (bulky volumes <5 cm^3), were used, avoiding any changes in the natural distribution of the porous space and then dried for 24 h in a vacuum oven at ~70 °C. Data were processed by SOL.I·D (Solver of Intrusion Data), software (Ver. 1.6.6. – Thermo Scientific), allowing to determine real and bulk densities, Hg open porosity, total pore surface area, and average, median, and modal pore radius. Three measurements were the minimum number of average data for pore size distribution curve.

2.5. Thermal analyses

Powdered starting geomaterials were analyzed by means of simultaneous thermal analyses, namely thermogravimetry (TG) and differential scanning calorimetry (DSC), using a NETZSCH STA 449 F3 Jupiter thermoanalyzer, in alumina crucibles. Samples underwent to a dynamic heating conditions (heating rate 10 °C/min, 40–1250 °C range) in ultrapure air. Proteus 6.1.0 software was used for data analysis.

2.6. Fourier Transform Infrared spectroscopy

Fourier transform infrared spectroscopy (FTIR) was performed on powdered samples in Attenuated Total Reflectance mode (ATR) using a BRUKER Alpha FTIR spectrometer equipped with a diamond crystal (Mid-Infrared spectral range 4000–400 cm^{-1}; spectral resolution 4 cm^{-1} and 64 scans for each run). Spectra were acquired and processed with the software Opus 7.8.44.

2.7. Lightweight Expanded Aggregates production

Firing behavior was evaluated by a preliminary test using a Hot-Stage Microscope (HSM - Expert System Solutions - Misura 2) on cylindrical specimens (2 mm diameter, 3 mm height) treated with a heating rate of 10 °C/min until melting (Dondi et al., 2001). Once operative conditions (mainly temperature and firing time) were identified by means of HSM, a laboratory scale simulation of Lightweight Expanded Aggregates (LEA) production was conducted by preparing pellets (40 mm in diameter, pressed at 40 MPa and then hand-granulated to 3-10 mm in size). The resulting granulate was fired in an electric chamber kiln (Nannetti mod. CV). Operative conditions are consistent with previous experimental research on zeolite-rich materials (de Gennaro et al., 2004, 2007, 2008, 2009; Graziano et al., 2022).

Physical and technological properties of LEA were tested by determining: particle size distribution (UNI EN 13055, 2016), bulk density by Archimede's principle (UNI EN 13055, 2016), loose bulk density (UNI EN 13055, 2016), strength of particle using a Control Test and 1 $MPa*s^{-1}$ as load rate, (average value from 20 tests) and water absorption (UNI EN 13055, 2016).

Based on bulk chemistry and mineralogical properties of the fired LEA, chemical composition and structural parameters of the glassy phase were calculated. The chemical composition was defined by subtracting from the bulk chemistry of the fired body the contribution of mineralogical phases, assuming their stoichiometric composition weighted on the quantitative phase analysis. Shear viscosity at high temperature was estimated by a predictive model based on the chemical composition of the liquid phase (Giordano et al., 2008) while pseudo-structural parameters were calculated as follows:

Degree of depolymerization of the melt (NBO/T) defined as the number of Non-Bridging Oxygens (NBO) per tetrahedrally coordinated cations (Si, Al) as atomic percentage and calculated from the composition of the vitreous phase.

Glass network formers (GNF) - From the composition of the liquid phase: GNF (atom%) = Si + CCAT, corresponding to Al^{3+} charge compensated by alkali or alkaline earths.

Charge compensated aluminum in tetrahedral coordination (CCAT) - From the composition of the liquid phase: Al^{3+} charge compensated by alkali and alkaline earths: CCAT(atom%) = Na + K + 2Ca + 2 Mg (up to max value = Al).

Glass network modifiers (GNM) - From the composition of the liquid phase: alkali and alkaline earths exceeding CCAT: GNM (atom%) = Na + K + 2 Mg + 2Ca – CCAT.

2.8. Pozzolanic activity

The pozzolanic activity was evaluated using a standard chemical method, accepted as European Standard (Fratini, 1949, 1950; UNI EN 196-5, 2015). Firstly, tuff-cement blends were prepared by mixing in a mortar, 13 g of Portland cement (OPC, CEM I) with 7 g of each tuff sample, in such a way tuff was 35% by weight of the binder. Afterwards, the above tuff-cement blends were mixed with 100 mL of boiled deionized water, stored at 40 °C in 500-mL cylindrical polyethylene containers. Samples so prepared were kept at 40 °C for 8 or 15 days (if the test was negative after 8 days). At the end of the experiment, Ca^{2+} and OH^- concentrations in the contact solution are estimated using volumetric analysis methods (i.e., complexometric titration with ethylenediaminetetraacetic acid-EDTA and acid-base titration, respectively).

Collected data (i.e., the average values of runs performed in triplicate) were reported in a plot of $Ca(OH)_2$ (expressed as CaO) solubility at 40 °C as a function of OH concentrations in solution (i.e., vs. alkalinity). Points representing under-saturated solutions, and thus proving the existence of pozzolanic activity given by the specific mineral addition to the OPC, should be under the curve, which means that some of the lime resulting from the hydrolysis of the clinker was fixed by the pozzolanic materials. On the contrary, points above and on the curve represent

over-saturated and saturated solutions, respectively, indicating the lack of pozzolanic activity.

Data collected from Fratini's plot can be analyzed using the following equation: $CaO_T = (350/[OH]-15)$, representing the theoretical solubility data of $Ca(OH)_2$ (as CaO) at 40 °C in the 35–90 mmol/l [OH−] range. To collect further information about the kinetic of the pozzolanic reaction, data were also collected at longer time up to 21 days.

2.9. Cation exchange capacity, external cation exchange capacity, Zeta potential and drug loading test

Exchangeable cations (i.e., Na^+, K^+, Mg^{2+}, and Ca^{2+}) were extracted using the batch exchange method (BEM) in order to assess the cation exchange capacity (CEC) of the examined geomaterials (Cappelletti et al., 2017). In particular, 1 g of powdered tuff was mixed with 35 mL NH_4Cl solution (1 M) in nalgene tubes at constant temperature (60 °C). The solid was separated by centrifugation each 2 h and the exhausted solution was replaced with other 35 mL of fresh solution. After at least ten runs, the solutions were examined in atomic absorption spectrometry (AAS) and concentration of cations were estimated in meq/g.

The concentrations of the same exchangeable cations were determined also after continuous stirring of 2.5 g of powdered tuffs with 30 mL of cetylpyridinium chloride (CP-Cl) solution (20 mM) for 24 h in order to evaluate the external cation exchange capacity (ECEC) of the examined geomaterials (Cappelletti et al., 2017). The solutions were extracted by centrifugation and then analyzed by means of atomic absorption spectrophotometry. ECEC was evaluated from the liquid and expressed in meq/g. After interaction, the powdered tuff was filtered and washed in order to remove the unnecessary surfactant and dried at room temperature. This procedure allowed also to obtain, at the same time, a surface modified natural zeolite (SMNZ) to perform preliminary drug loading tests (i.e., equilibrium sorption isotherm). For this purpose, 25 mL of ibuprofen sodium salt (IBU), having concentrations ranging between 50 and 1000 mg/L, were stirred with 0.1 g of SMNZ for 5 h. Then the solutions were extracted by centrifugation and analyzed by means of a Shimadzu UV-VIS spectrophotometer. Absorbance was measured at $\lambda = 222$ nm. Experimental data were fitted using the Langmuir equation one of the most used mathematical models $S=S_m(KC_e/1 + KC_e)$ (Langmuir, 1917): where S is the amount of IBU sorbed by SMNZ at equilibrium conditions (values expressed in mg/g); S_m is the maximum sorption capacity of SMNZ at equilibrium (mg/g); C_e the concentration of IBU in the solutions at the equilibrium (mg/L); K is a constant (the so-called Langmuir coefficient) expressed in L/mg and related to adsorption intensity and binding energy. S_m and K were estimated from the slope and intercept of the linearized Langmuir equation (plot C/S vs. C). The correlation coefficient R^2 was used to evaluate the applicability of the Langmuir model.

Zeta potential can be determined only on the nanometric fraction of zeolite samples using a Zetasizer Ultra apparatus (Malvern, USA). Before measurements, 50 mL of an aqueous suspension of micronized C1 and P2 samples were prepared (5 mg/mL) and placed on a flat surface. Subsequently, 10 μL aliquots were withdrawn immediately below the suspension surface and poured in 1 mL of DDW. Then, 780 μL of the obtained suspension were placed in NanoSizer cuvette to run the experiments.

3. Results and discussion

3.1. Raw materials characterization

3.1.1. Mineralogical and chemical composition

The mineralogical composition consists of zeolites (almost exclusively chabazite and minor phillipsite and analcime) along with K-feldspar, mica, plagioclases, and pyroxenes (Table 1). Only for sample C1, the presence of calcite is detectable and reported also in literature (Gualtieri et al., 1999). The chemical composition is consistent with mineralogy (Table 1). In particular, it is evident the high potassium content that is a peculiar feature of VVD magmas. Sample C1 has a slightly higher value of CaO due to the occurrence of calcite. All samples (products and waste) have a very similar composition, and, even if, the two waste materials (C2 and P2) exhibit slightly higher values of the total zeolite content (TZC), this circumstance is probably related to a particle size segregation of the powder, which in certain way promotes a zeolite enrichment. At any event, a high zeolites content is beneficial for technological applications.

Table 1
Mineralogical and chemical composition (tr = traces).

	Unit	C1	C2	P1	P2
chabazite	wt%	49	52	51	58
phillipsite		3	2	1	2
analcime		tr	tr	1	1
K-feldspar		17	16	18	14
plagioclase		4	2	3	2
pyroxene		5	4	5	4
mica		3	4	3	3
calcite		2	tr	tr	tr
amorphous		15	18	17	17
TZC		53	55	54	61
SiO_2	wt%	49.3	49.9	50.2	49.8
TiO_2		0.5	0.5	0.5	0.5
Al_2O_3		14.9	15.7	15.3	15.4
Fe_2O_3		3.6	3.6	3.6	3.3
MnO		0.1	0.1	0.1	0.1
MgO		1.4	1.4	1.5	1.4
CaO		6.3	5.6	5.5	5.8
Na_2O		0.5	0.5	0.5	0.4
K_2O		6.2	5.0	6.1	5.4
P_2O_5		0.1	0.1	0.2	0.1
Loss on Ignition	%	16.5	17.0	15.7	17.1

3.1.2. Scanning Electron Microscopy – Energy Dispersive Spectrometer microanalyses

Scanning electron observations on rock samples highlighted the presence of euhedral crystals: firstly zeolites (mainly chabazite along with minor phillipsite), smectite and volcanic glass as main constituents in samples quarry C and quarry P (Fig. 1) as also reported in literature as typically constituting this rock type. Zeolites, in this volcanic deposit, form by means of post-depositional minerogenetic processes that led to the crystallization of minerals from volcanic glass (Sparks, 1975; Langella et al., 2013b; Colella et al., 2017). Usually, this process, happens at temperatures between 120 and 230 °C, too low for feldspatization but suitable for zeolitization and by a deep interaction between fresh volcanic glass and meteoric water (Laurenzi and Villa, 1987; Cappelletti et al., 2003; Giampaolo et al., 2008; Fedele et al., 2008; Bear et al., 2009; Langella et al., 2013). Fluids circulation of these waters to leads hydrolysis and dissolution of the glass itself with the formation of a chemical and thermodynamic environment suitable for zeolites crystallization.

EDS investigations, performed on *juvenile* elements (volcanic glass), confirmed sample's petrographical classification as phonolites and trachytes in the T.A.S. diagram (Le Bas et al., 1986 - Appendix, fig. A1) with a Si/Al ratio always higher in the glasses than in the derived authigenic phases.

3.1.3. Mercury intrusion porosimetry results

Porosimetric investigations were performed to acquire a complete basic characterization of this macroporous tuff and compared with that of other Italian pyroclastites used as raw material for similar technological applications (de Gennaro et al., 2005, 2007; Cappelletti et al., 2011; Izzo et al., 2022) (Appendix – Table A1). Both samples exhibit high accessible porosity values (Table 2). The pore size curves reported a unimodal distribution with predominance of macropores (97%) for

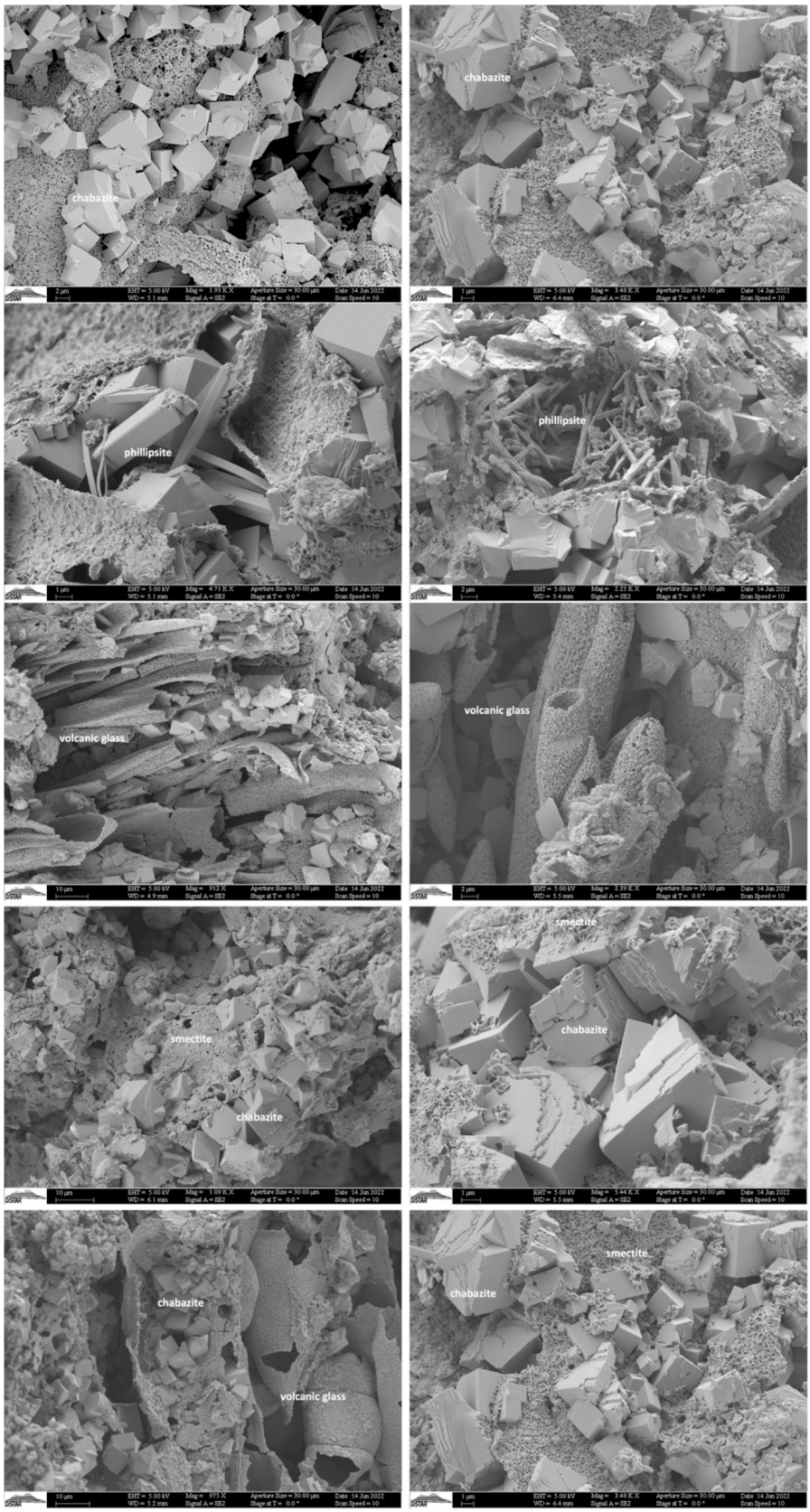

Fig. 1. SEM micrographs of C and P samples (left and right column respectively).

Table 2
Porosimetric features.

	Unit	C1	P1
Bulk density	g/cm^3	1.3	1.1
Apparent density	g/cm^3	2.3	2.1
Accessible porosity	%	42.6	48.7
Total pore volume	mm^3/g	325.3	446.0
Total pore surface area	m^2/g	8.3	8.9
Average pore diameter	mm	0.2	0.2
Median pore diameter	mm	1.4	1.8

both, with pore diameter centered in modal class of 2 μm and 2.7 μm, respectively (Appendix – fig. A2). Mesopores are poorly represented. Dataset were in line with those of geomaterials of similar geological origin (Appendix – Table A1) (Chiodi et al., 1982; Bianchetti et al., 1990; Fratini et al., 1990; Jackson et al., 2005; De Casa and Lombardi, 2007; de Gennaro et al., 2013).

3.1.4. Thermal behavior

Thermal behavior of examined geomaterials can be schematically described by three different thermal events occurring: 1) from room temperature to 550 °C, 2) between 550 and 800 °C, 3) up to the final temperature of 1050 °C (Table 3). The most peculiar response of the zeolite-rich material happened during the first thermal range, consisting of an endothermic dehydration due to the release of the so-called zeolitic water contained in the cages and channel characterizing zeolite frameworks. The weight losses (ΔW), estimated by thermogravimetry are lower in lithoid samples (C1 and P1) rather than powdered ones (C2 and P2). This results generally suggest an increase of zeolite content in the waste produced by quarries operations. In the thermal range 550–800 °C, there is a weight loss representative of the decomposition of carbonates (i.e., calcite) for sample C1, and absent or as traces in the remaining samples. At higher temperatures (800–1050 °C), DSC analysis highlights an exothermic thermal event attributable to a sintering process. Residual mass (R.M.) values, in accordance with TZC and previous considerations are lower for waste samples.

3.1.5. Infrared spectroscopic features

ATR-FTIR spectra of chabazite-rich tuffs from Sorano Formation are reported in Appendix – fig. A3. FTIR and revealed the main spectral features for samples C1, C2, P1 and P2. All these samples showed a very strong band, representative of the asymmetric stretching vibrations of T-O bond, close to 998 cm^{-1}. The asymmetric and symmetric stretching vibrations in T-O-T bonds are represented by the moderate absorption bands at ~762 and 720 cm^{-1}. These three bands are generally diagnostic for chabazite since associated to the internal and external framework vibrations of Primary and Secondary Building Units (Karge, 2001; Byrappa and Kumar, 2007; Mozgawa et al., 2011; Izzo et al., 2019). The broader and weaker bands at ca. 3400 and 1640 cm^{-1} confirm the presence of zeolitic water (including hygroscopic one) and could be shared by chabazite and other phyllosilicates (i.e., smectite), along with the minor bands at 1120, 628, 516 and 460 cm^{-1}. Additional bands at 1455 and 874 cm^{-1}, in sample C1, are respectively attributable to asymmetric C—O and out-of-plane vibrations in calcite (Adler and Kerr, 1962; Vahur et al., 2016; Mercurio et al., 2018).

Table 3
Simultaneous thermal analyses ((a). Endothermic; (b). Exothermic; ΔW. weight loss by TG).

		Unit	C1	C2	P1	P2
$T < 550$ °C	ΔW	%	11.6	14.8	12.2	14.5
	DSC (a.b)	°C	154 (a) ÷ 232 (a)	149 (a) ÷ 231 (a)	132 (a) ÷ 240 (a)	134 (a)÷224 (a)
550 °C < T < 800 °C	ΔW	%	2.3	0.1	0.2	0.1
	DSC (a.b)	°C	668 (a)	–	–	–
800 °C < T < 1050 °C	ΔW	%	–	–	0.1	–
	DSC (a.b)	°C	905 (b)	891 (b)	898 (b)	901 (b)
	R.M	%	87.4	84.8	87.4	85.4

3.2. Technological characterization

3.2.1. Lightweight expanded aggregates production and characterization

Waste powders were crude pelletizzed by a 400 kg/cm^2 pression by a manual pneumatic press and then hand granulated (Fig. 2 a,b). Firing conditions were set to be consistent with the geomaterial thermal behavior (Table 3) and following suggested temperatures from Hot Stage Microscope (HSM) results (Table 4).

The firing schedule (maximum temperature 1250 °C with 5 min dwell time) was selected as intermediate between the Tme and Tmve temperatures (Table 4), according to previous studies (de Gennaro et al., 2007, 2009). The maximum volume expansion potentially achievable (from 80% to 97%) is adequate for LEA manufacturing. Applying this firing schedule to LEA prototypes, a similar appearance was obtained for both samples (Fig. 2c,d,e) and bulk density below 1000 kg/m^3 (Table 5). For this reason, they match the standard definition of "expanded lightweight aggregate" (UNI EN 13055, 2016).

The phase composition of such waste-based LEAs consists of a predominant vitreous phase associated to residual K-feldspar and plagioclase (Table 5). In these cases, both bulk viscosity and bloating index are mainly controlled by the chemical composition of the vitreous phase that was studied along with its physical properties (Kaz'mina, 2010).

The samples have similar phase composition and features of the vitreous phase. The fact that LEAs must be predominantly glassy with a limited skeleton, and a viscosity high enough to maintain the spheroidal shape, is well known (Cougny, 1990). However, literature data are only available for LEA obtained from zeolitic rocks mixed with glass waste (Dondi et al., 2016). In this case, the vitreous phase was slightly larger (83-90%) with less residual feldspars and quartz than in the present study. The shear viscosity was in the 3.3-3.7 $\log_{10}$ Pa·s range, i.e. fully comparable with reported data (~3.1 $\log_{10}$ Pa·s) considering that firing at lower temperatures (1110–1210 °C range, Dondi et al., 2016) implies a viscosity higher than at 1250 °C (Table 5).

The P2-based LEA has a slightly lower viscosity than C2, essentially because of its higher amount of glass network modifiers. The calculated viscosity values are in accordance with the bulk density achieved for the fired specimens, given by a different expansibility. In both cases, the shear viscosity is in accordance with the optimal range for lightweight aggregates production reported in literature (Molinari et al., 2020; Graziano et al., 2022).

Both waste-based LEAs were studied from the microstructural point of view, by means of SEM observations, in terms of quantity and quality of both pores and septa constituting the internal expanded structure (Appendix- fig. A4).

Micrographs show that bloating induced the formation of a bimodal pores' classes: a first population with bubbles diameter > 400 μm and a second one with bubbles diameter < 150 mm (Table 6).

The two specimens have comparable microstructural features, and, for both, the formation of an external glassy surface plays a key role for a possible use in the concrete industry (Mueller et al., 2008; de Gennaro et al., 2009; Volland and Brötz, 2015; Graziano et al., 2022).

Such a surface determines a low aggregates water absorption allowing, on the other hand, to keep down the water-cement ratio that can be detrimental (if too high) for good concrete formulations (Lo et al., 2007; Collepardi et al., 2016). Experimentally produced LEAs were characterized from the physical-mechanical point of view and achieved values were compared to those of some commercial products with a similar bulk density value (Table 7, Appendix - Table A2).

As the other reported commercial products and as other waste-based LEA, aggregates manufactured in this research offer a remarkable range

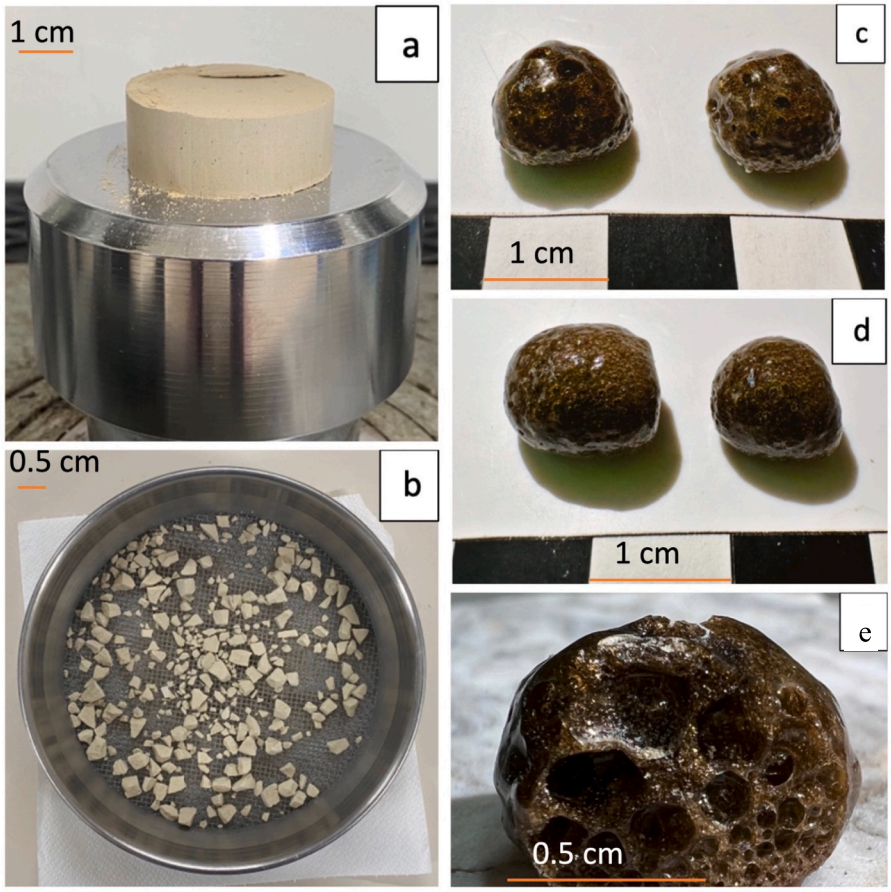

Fig. 2. LEAs produced from C and P. Crude pelletization (a), crude hand-graining (b), fired cooling (c: C2-based LEA; d: P2-based LEA), internal structure (e).

Table 4
Hot Stage Microscope (HSM) results.

	Unit	C		P	
		C1	C2	P1	P2
Sintering temperature (Ts)	°C	1156	1134	1156	1158
Softening temperature (Tr)	°C	1186	1170	1172	1208
Melting temperature (Tf)	°C	1346	1372	1344	1342
Temperature of maximum expansion (Tme)	°C	1240	1260	1290	1260
Temperature of max expansion rate (Tmve)	°C	1210	1218	1210	1220
Maximum volume expansion at Tme	%	80	97	80	82
Bloating index	unit	0.8	1.1	0.8	0.9

of physical characteristics (e.g., bulk density and water absorption) and processing conditions (e.g. firing behavior) and they are completely usable for building sector.

Furthermore, considering the production of lightweight aggregates, which is the application with the highest impact for raw material consumption, with regard to the life cycle assessment (LCA) simulation the production of zeolite-rich waste-based aggregates present a significantly lower environmental burden with respect to the production of commercial ones, mainly due to potential benefits of avoided impact from raw materials extraction, transportation and the production phase (including burning and expansion with heavy fuel oil). Even when used in the mix design of 1 m^3 of lightweight concrete with C20/25 strength class and 1600 kg/m^3 of density, waste-based aggregates present a lower impact in all the damage and impact categories (Napolano et al., 2016).

Table 5
LEA: firing temperatures; mineralogical, chemical and physical characterization.

	Unit	C	P
Firing temperature	°C	1250	1250
Bulk density	kg/m^3	920	990
K-feldspar	wt%	12	13
Plagioclase		10	9
Vitreous phase		78	78
SiO_2	wt%	55.4	56.4
TiO_2		0.7	0.8
Al_2O_3		19.2	19.5
Fe_2O_3		5.4	5.4
MgO		2.1	2.3
CaO		9.4	8.2
MnO		0.2	0.2
P_2O_5		0.2	0.3
Na_2O		0.7	0.8
K_2O		6.7	6.3
Shear viscosity	Log_{10} Pa s	3.1	3.1
Flow point	°C	1145	1152
NBO/T[1]	unit	0.1	0.1
GNF[2]	atom%	28.3	28.6
CCAT[3]		8.21	8.3
GNM[4]		4.9	3.9

[1] Number of Non-Bridging Oxygens per Tetrahedrally-coordinated cations.
[2] Glass network formers.
[3] Charge compensated aluminum in tetrahedral coordination.
[4] Glass network modifiers.

Table 6
LEA: microstructural investigations.

Surface aspect	Unit	C	P
		glassy	glassy
Pores 1st population	mm	700–1000	400–1100
Pores 2st population		40–100	55–120
Septa		50–300	100–450
Pores shape – distribution		Rounded – homogeneus	Elongated – homogeneus

Table 7
LEA: physical-mechanical characterization.

	Unit	C	P
Particle size distribution	mm	03–10	03–10
Bulk density	kg/m^3	920	990
Loose bulk density		660	515
Water absorption (24 h)	%	3	2.93
Strength of particle	MPa	0.3	0.3

3.2.2. Pozzolanic activity

The evaluation of the reactivity as pozzolanic materials of the analyzed tuffs have been reported in Fig. 3. As expected, all the investigated samples provide undersaturation conditions (Liguori et al., 2015, 2019; Özen et al., 2016; Montesano et al., 2022), being positioned under the equilibrium $Ca(OH)_2$ solubility curve. This means that zeolites (i.e., pozzolanic materials) react with calcium hydroxide, leading to the formation of insoluble calcium aluminate silicate hydrate (C-A-S-H) (acting as binding compounds). In fact, zeolites interacting with the solution modify its chemistry, decreasing Ca^{2+} concentration and increasing alkalinity. Starting from the empirical formula (see equation chapt. 2), it is possible to quantify the pozzolanic activity of the investigated samples. The results of these calculations are reported in Table 8. The reduction of $Ca(OH)_2$ in terms of CaO, can be calculated as pozzolanic activity index PA (%) = $[(CaO_T - CaO)/ CaO_T]*100$.

The examined samples, C and P, displayed a high reactivity with lime, reaching a PA of 82.8% and 69.8% respectively. Inspecting data at longer times (Fig. 3) the maximum percentage of $Ca(OH)_2$ reduction was attained after 21 days.

For this reason, waste here investigated could be used as an active additive and a partial substitute in compounds to lower the amount of cement used and by consequence contributing to lower also the CO_2 footprint up to 20% as demonstrated in recent studies aimed to partially replacing cement with technologically interesting materials (Damtoft et al., 2008; Huntzinger and Eatmon, 2009; Van Den Heede and De Belie, 2012; Miller et al., 2018; Shah et al., 2022; Her et al., 2024; Tokareva et al., 2024).

Table 8
OH and CaO concentrations and CaOT and PA evaluations (OH and CaO taken from the $Ca(OH)_2$ solubility curve; CaOT and PA result from the formulas).

	Unit	C			P		
		8 days	15 days	21 days	8 days	15 days	21 days
OH^-	mmol/	42.7	48.2	50.0	42.2	44.3	42.2
[CaO]	L	2.2	1.2	0.93	3.9	1.5	1.3
$[CaO]_T$		12.6	10.5	10.1	12.8	11.9	12.8
PA	%	82.8	89.0	90.7	69.8	87.3	89.8

3.2.3. Surface modification, Zeta (ζ) potential and drug sorption

Zeta potential (ZP) measurements allowed the detection of the net surface charge of samples in the presence/absence of the surface-active agent starting from measuring the electrophoretic mobility of the colloidal fraction of waste powder.

The detected ZP values of colloidal particles, the addition of a cationic surfactant (surfactant modified samples, respectively C_T and P_T), led to a positive shift in ZP of particles, confirming the superficial charge inversion (Table 9, Fig. A5).

This finding suggests a significant affinity between the surfactant molecules and, hence, that surfactant does adhere to the zeolite particles in the colloidal size scale. Furthermore, it is worth noting that the C_T sample exhibited a higher ZP than P_T, thereby hinting at a more effective shielding effect of the colloidal zeolite suspension.

To, preliminarily, evaluate technological performance of chabazite-rich rock from Sorano Formation in the uptake of non-steroidal anti-inflammatory drug (NSAID), the functionalized geomaterial (waste) obtained after interaction with CP-Cl was tested by means of equilibrium sorption test using IBU solutions (Fig. 4).

Chabazite-rich rock from Sorano Formation functionalized with CP-Cl has a maximum sorption capacity $Sm \approx 10.6$ mg/g ($K = 0.0834$ L/meq; $R^2 = 0.997$). The asymptotic shape of the equilibrium isotherm suggests a favorable sorption of IBU by the examined geomaterials after surface modification. Taking into the account the total zeolite content of these geomaterials, the results here obtained could be considered quite consistent with data from literature for chabazite- and phillipsite-rich geomaterials (Serri et al., 2016; Mercurio et al., 2018; Izzo et al., 2019). Zeolite content could influence the surfactant sorption capacity (i.e., ECEC value) of starting geomaterial and consequently the performance of SMNZ on the uptake of NSAIDs. Geomaterials modified with

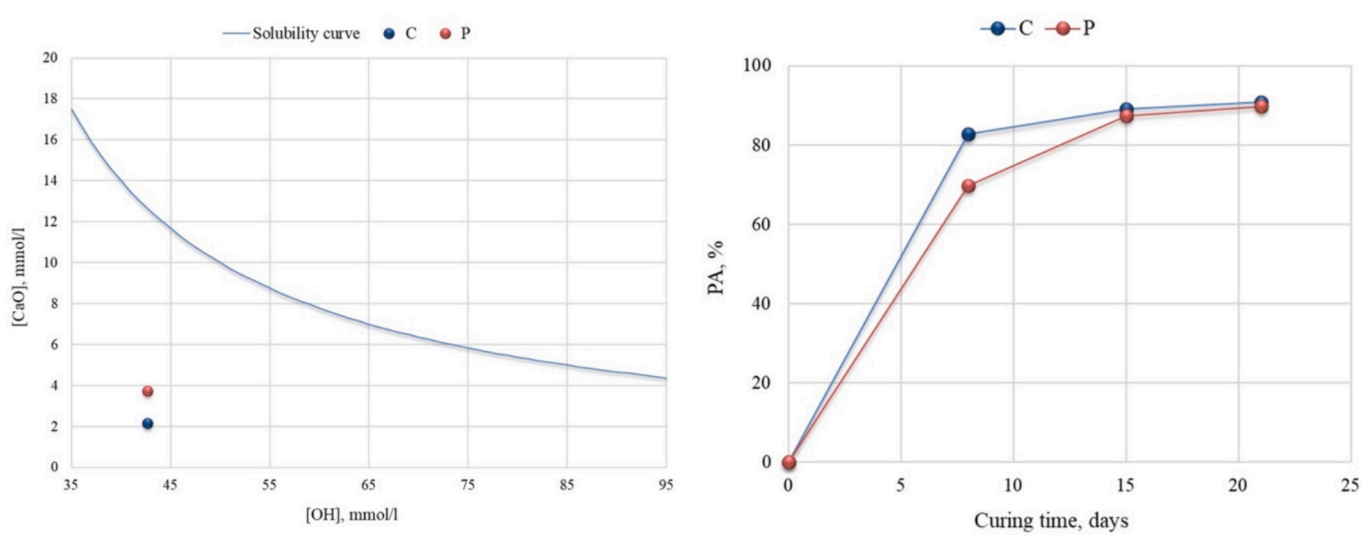

Fig. 3. Results of Fratini's test. Solid lines represent $Ca(OH)_2$ solubility curve (left) and Pozzolanic reactivity percentage as a function of curing time (right).

Table 9
CEC, ECEC and Zeta Potential values.

	Unit	C1	C2	P1	P2
CEC					
K^+	meq/g	0.5	0.6	0.5	0.6
Na^+		0.1	0.1	0.1	0.1
Ca^{2+}		1.6	1.5	1.1	1.3
Mg^{2+}		0.1	0.2	0.2	0.2
Tot.		2.3	2.4	1.9	2.2
ECEC	meq/g		<0.06		<0.06
		bare	surfactant modified (C_T)	bare	surfactant modified (P_T)
ζ Potential	mV/total counts	−25.2 ± 3.4	23.8 ± 1.28	−37.1 ± 2.8	18.6 ± 2.53

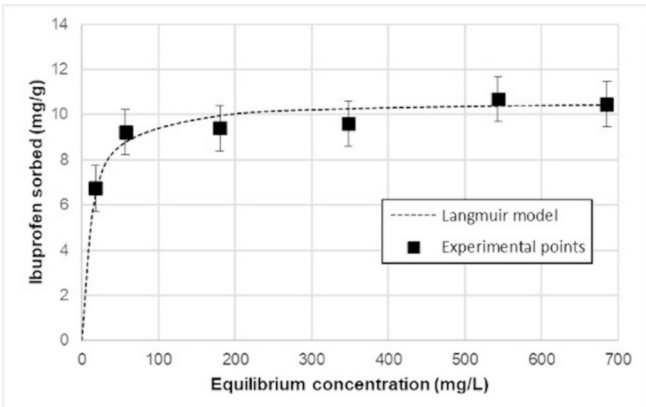

Fig. 4. Ibuprofen sodium salt sorption equilibrium isotherm in chabazite-rich rock from Sorano Formation surface modified with CP-Cl.

chlorinated surfactants such as CP-Cl, but also benzalkonium chloride or hexadecyltrimethylammonium chloride, form onto the surface of natural zeolite a patchy bilayer that led to a complex sorption process characterized by a predominant external anion exchange of drugs molecules and a subordinate partition into the hydrophobic portion of micelle. The hydrophobicity and molecular conformation of both surfactant and drug also play a significant role in the technological performance of SMNZs. Previous investigations demonstrate that natural zeolite functionalized with hexadecyltrimethylammonium chloride can sorb higher concentration of NSAIDs. Nevertheless, CP-Cl is considered more suitable for pharmaceutical preparations (Serri et al., 2016; Mercurio et al., 2018; Izzo et al., 2019).

For the same SMNZs, different performances can be noticed as a function of the type of drug. For example, the concentration of diclofenac sodium that can be sorbed by a SMNZ is generally twice than ibuprofen because of the higher hydrophobicity and minor steric hindrance of diclofenac that can be trapped more easily into the internal portion of micelle (Pasquino et al., 2016).

In the light of these first results, the NSAID sorption capacity of surfactant modified chabazite-rich geomaterials form Sorano Formation hardly seems adequate for a real pharmaceutical application. However, further investigations are required although the technological performance of these geomaterials appear likely compatible for environmental applications such as the removal of some NSAIDs from waste waters, often considered in the last years as contaminants of emerging concern (Izzo et al., 2019).

4. Conclusions

Zeolite-rich rocks can be excellent raw materials for various uses, but sustainability of mining operations needs to be enhanced by improving resource efficiency. For this purpose, the chance of upgrading with profit a quarry waste into a by-product utilized in high-profile technological applications is a game changer concept even though it requires a specific technological characterization.

This research has demonstrated the feasibility of using a zeolite-rich quarry waste (collected from the Sorano formation) in various applications, such as the production of lightweight expanded aggregates (LEA), the pozzolanic addition in the production of cement and the possibility to act as carrier for pharmacologically active molecules. This is a step forward to prevent landfill disposal of about 40% of the volcaniclastic deposit.

Lightweight aggregates with water absorption below 3% and density of 920-990 kg/m^3 are pretty in line with the products on the marketed. In addition, these LEAs can play an important role in concrete mix design as absolutely not detrimental to the water-cement ratio. Waste-based LEA can therefore be considered a good candidate for the manufacturing of lightweight concretes, contributing to improve thermal and acoustical insulation.

The zeolite-rich waste reacts with calcium hydroxide, leading to the formation of insoluble calcium aluminate silicate hydrate, and acting as binding compound. Its pozzolanic activity qualifies the material as suitable to produce cement mixtures with satisfactory mechanical strength. Tested samples provided undersaturation conditions with the maximum percentage of $Ca(OH)_2$ reduction (around 91%) attained after 15 days.

Although the technological performance of these geomaterials appears compatible for environmental applications, such as the removal of some NSAIDs from waste waters, often considered in the last years as emerging contaminants, further investigations are required. Surface charge reversion of the superficial modified samples, going from -30 to +20 mV/TotCount (average ζ-potential values), allowed an early uptake of non-steroidal anti-inflammatory drugs, even if low values of ECEC (0.06 meq/g) along with a maximum sorption capacity $Sm \approx 10.6$ mg/g hardly seem adequate for a real pharmaceutical application.

According to results reported in the present research, zeolite-rich waste can be used as secondary raw material, representing a green alternative to the disposal. By this way, low grade natural resources, such as volcaniclastic deposits, can play a more important role as useful and versatile technological materials, enhancing the economies of territories and the industrial development, also from an environmental perspective. Therefore, this study should also spur stakeholders to promote new combined applied research approaches that can raise funding from both the private and public sectors.

CRediT authorship contribution statement

Sossio Fabio Graziano: Writing – review & editing, Writing – original draft, Validation, Supervision, Resources, Methodology, Investigation, Data curation, Conceptualization. **Mariano Mercurio:** Writing – review & editing. **Francesco Izzo:** Writing – review & editing, Investigation. **Alessio Langella:** Writing – review & editing. **Concetta Rispoli:** Writing – review & editing. **Nicola Davide Santaniello:** Investigation. **Claudia Di Benedetto:** Investigation. **Vincenzo Monetti:** Investigation. **Marco Biondi:** Writing – review & editing. **Giuseppe De Rosa:** Writing – review & editing. **Laura Mayol:** Writing – review & editing. **Fabrizio Villapiano:** Writing – original draft, Investigation. **Michele Dondi:** Writing – review & editing. **Chiara Molinari:** Writing –

review & editing. **Barbara Liguori:** Writing – review & editing. **Assunta Campanile:** Investigation. **Piergiulio Cappelletti:** Writing – review & editing, Supervision, Conceptualization.

Declaration of competing interest

The authors declare that they have no known competing financial interests or personal relationships that could have appeared to influence the work reported in this paper.

Data availability

No data was used for the research described in the article.

Acknowledgements

Authors would like to express their great thanks to Dr. Alfredo Granato for his kindness and helpfulness in providing the samples. Francesco Izzo was supported by a research grant on the project PON "Ricerca e Innovazione" 2014-2020 (PON R&I) - Azione IV.6 – "Contratti di ricerca su tematiche Green"; CUP: E65F21003260003. Open Access funding provided thanks to University Federico II CARE/CRUI agreement with Elsevier.

References

Adler, H.H., Kerr, P.F., 1962. Infrared study of aragonite and calcite. Am. Mineral. 47, 700–717.

ASTM International, 2021. ASTM D7348-21 Standard Test Methods for Loss on Ignition (LOI) of Solid Combustion Residues.

Banaszak, M., Biesek, J., Adamski, M., 2022. Aluminosilicates at different levels in rye litter and feed affect the growth and meat quality of broiler chickens. Vet. Res. Commun. 46, 37–47. https://doi.org/10.1007/s11259-021-09827-x.

Bareschino, P., Pepe, F., Diglio, G., 2017. Modelling of a zeolite-rich tuff desiccant wheel. Adv. Sci. Lett. 23, 6002–6006. https://doi.org/10.1166/asl.2017.9092.

Bareschino, P., Pepe, F., Roselli, C., Sasso, M., Tariello, F., 2019. Desiccant-based air handling unit alternatively equipped with three hygroscopic materials and driven by solar energy. Energies (Basel) 12. https://doi.org/10.3390/en12081543.

Bear, A.N., Giordano, G., Giampaolo, C., Cas, R.A.F., 2009. Volcanological constraints on the post-emplacement zeolitisation of ignimbrites and geoarchaeological implications for Etruscan tomb construction (6th-3rd century B.C) in the Tufo Rosso a Scorie Nere, Vico Caldera, Central Italy. J. Volcanol. Geotherm. Res. 183, 183–200. https://doi.org/10.1016/j.jvolgeores.2009.03.016.

Belkin, H.E., Rolandi, G., Jackson, J.C., Cannatelli, C., Doherty, A.L., Petrosino, P., De Vivo, B., 2016. Mineralogy and geochemistry of the older (40 ka) ignimbrites on the Campanian Plain, southern Italy. J. Volcanol. Geotherm. Res. 323, 1–18. https://doi.org/10.1016/j.jvolgeores.2016.05.002.

Bianchetti, P.L., Lombardi, G., Marini, S., Meucci, C., 1990. The volcanic rocks of the monuments of the Forum and Palatine (Rome): characterization, alterations, and results of chemical treatments. In: Charola, A.E., Koestler, R.J., Lombardi, G. (Eds.), Proceedings of the International Meeting on Lavas and Volcanic Tuffs, Easter Island, pp. 83–105.

Biesek, J., Dunisławska, A., Banaszak, M., Siwek, M., Adamski, M., 2021. The impact of hydrated aluminosilicates supplemented in litter and feed on chicken growth, muscle traits and gene expression in the intestinal mucosa. Animals 11. https://doi.org/10.3390/ani11082224.

Bogusz, A., Tomczyk, B., Trzcińska, M., Mirosław, B., Gworek, B., 2024. Effect of zeolites on the reduction of the ecotoxicity of carbamazepine in the environment. Ecotoxicol. Environ. Saf. 277 https://doi.org/10.1016/j.ecoenv.2024.116320.

Brumovská, V., Šorf, M., Mareš, J., 2021. The effect of clinoptilolite as a feed additive on selected rainbow trout (*Oncorhynchus mykiss*) haematological and biochemical parameters, before and after stress treatment. Aquac. Res. 52, 3540–3548. https://doi.org/10.1111/are.15195.

Byrappa, K., Kumar, S.B.V., 2007. Characterization of zeolites by infrared spectroscopy. Asian J. Chem. 19 (6), 4933–4935.

Cappelletti, P., Langella, A., Colella, A., De Gennaro, R., 1999. Mineralogical and technical features of zeolite deposits from northern Latium volcanic district. Period. Mineral. 68, 127–144.

Cappelletti, P., Cerri, G., Colella, A., de' Gennaro, M., Langella, A., Perrotta, A., Scarpati, C., 2003. Post-eruptive processes in the Campanian Ignimbrite. Mineral. Petrol. 79, 79–97. https://doi.org/10.1007/s00710-003-0003-7.

Cappelletti, P., Rapisardo, G., De Gennaro, B., Colella, A., Langella, A., Graziano, S.F., Bish, D.L., De Gennaro, M., 2011. Immobilization of Cs and Sr in aluminosilicate matrices derived from natural zeolites. J. Nucl. Mater. 414, 451–457. https://doi.org/10.1016/j.jnucmat.2011.05.032.

Cappelletti, P., Petrosino, P., de Gennaro, M., Colella, A., Graziano, S.F., D'Amore, M., Mercurio, M., Cerri, G., de Gennaro, R., Rapisardo, G., Langella, A., 2015. The "Tufo Giallo della Via Tiberina" (Sabatini Volcanic District, Central Italy): a complex system of lithification in a pyroclastic current deposit. Mineral. Petrol. 109, 85–101. https://doi.org/10.1007/s00710-014-0357-z.

Cappelletti, P., Colella, A., Langella, A., Mercurio, M., Catalanotti, L., Monetti, V., de Gennaro, B., 2017. Use of surface modified natural zeolite (SMNZ) in pharmaceutical preparations Part 1. Mineralogical and technological characterization of some industrial zeolite-rich rocks. Microporous Mesoporous Mater. 250, 232–244. https://doi.org/10.1016/j.micromeso.2015.05.048.

Carbonchi, C., Dondi, M., Morandi, N., Tateo, F., 1999. Possible use of altered volcanic ash in ceramic tile production. Ind. Ceram. 19, 67–75.

Cataldo, E., Salvi, L., Paoli, F., Fucile, M., Masciandaro, G., Manzi, D., Masini, C.M., Mattii, G.B., 2021. Application of zeolites in agriculture and other potential uses: a review. Agronomy 11. https://doi.org/10.3390/agronomy11081547.

Chiodi, M., Nappi, G., Rossi, S., Volponi, E., 1982. L"ignimbrite di Orvieto nel quadro dell" evoluzione vulcano-tettonica dei Vulsini Orientali: Caratteristiche geologiche e tecniche. Boll. Soc. Geol. Ital. 101, 327–342.

Colella, A., Di Benedetto, C., Calcaterra, D., Cappelletti, P., D'Amore, M., Di Martire, D., Graziano, S.F., Papa, L., Langella, A., 2017. The Neapolitan Yellow Tuff: an outstanding example of heterogeneity. Constr. Build. Mater. 136, 361–373. https://doi.org/10.1016/j.conbuildmat.2017.01.053.

Collepardi, M., Collepardi, S., Troli, R., 2016. Il nuovo calcestruzzo, 6th ed. Enco srl.

Conticelli, S., Francalanci, L., Piero, M., Cioni, R., Sbrana, A., 1997. Petrology and geochemistry of the ultrapotassic rocks from the Sabatini Volcanic District, Central Italy: the role of evolutionary processes in the genesis of variably enriched alkaline magmas. J. Volcanol. Geotherm. Res. https://doi.org/10.1016/S0377-0273(96)00062-5.

Cougny, G., 1990. Spécifications sur les matières premières argileuses pour la fabrication de granulats légers expanses. Bull. Int. Assoc. Eng. Geol. 41, 47–55. https://doi.org/10.1007/BF02590206. Bulletin de l'Association Internationale de Géologie de l'Ingénieur.

Cucciniello, C., Melluso, L., le Roex, A.P., Jourdan, F., Morra, V., de' Gennaro, R., Grifa, C., 2017. From olivine nephelinite, basanite and basalt to peralkaline trachyphonolite and comendite in the Ankaratra volcanic complex, Madagascar: $^{40}Ar/^{39}Ar$ ages, phase compositions and bulk-rock geochemical and isotopic evolution. Lithos 274–275, 363–382. https://doi.org/10.1016/j.lithos.2016.12.026.

Damtoft, J.S., Lukasik, J., Herfort, D., Sorrentino, D., Gartner, E.M., 2008. Sustainable development and climate change initiatives. Cem. Concr. Res. 38, 115–127. https://doi.org/10.1016/j.cemconres.2007.09.008.

De Casa, G., Lombardi, G., 2007. Caratteri fisico-meccanici del Tufo Giallo della Via Tiberina (Roma). Rend. Fis. Acc. Lincei 18, 5–25.

de Gennaro, R., Cappelletti, P., Cerri, G., de' Gennaro, M., Dondi, M., Langella, A., 2004. Zeolitic tuffs as raw materials for lightweight aggregates. Appl. Clay Sci. 25, 71–81. https://doi.org/10.1016/j.clay.2003.08.005.

de Gennaro, R., Cappelletti, P., Cerri, G., De' Gennaro, M., Dondi, M., Langella, A., 2005. Neapolitan Yellow Tuff as raw material for lightweight aggregates in lightweight structural concrete production. Appl. Clay Sci. 28, 309–319. https://doi.org/10.1016/j.clay.2004.01.014.

de Gennaro, R., Cappelletti, P., Cerri, G., de' Gennaro, M., Dondi, M., Graziano, S.F.F., Langella, A., 2007. Campanian Ignimbrite as raw material for lightweight aggregates. Appl. Clay Sci. 37, 115–126. https://doi.org/10.1016/j.clay.2006.11.004.

de Gennaro, R., Langella, A., D'Amore, M., Dondi, M., Colella, A., Cappelletti, P., de' Gennaro, M., 2008. Use of zeolite-rich rocks and waste materials for the production of structural lightweight concretes. Appl. Clay Sci. 41, 61–72. https://doi.org/10.1016/j.clay.2007.09.008.

de Gennaro, R., Graziano, S.F., Cappelletti, P., Colella, A., Dondi, M., Langella, A., De' Gennaro, M., 2009. Structural concretes with waste-based lightweight aggregates: from landfill to engineered materials. Environ. Sci. Technol. 43, 7123–7129. https://doi.org/10.1021/es9012257.

de Gennaro, M., Calcaterra, D., Langella, A., 2013. Le pietre storiche della Campania - dall'oblio alla riscoperta. Luciano Editore.

de' Gennaro, M., Langella, A., 1996. Italian zeolitized rocks of technological interest. Mineral. Deposita 3, 472.

de' Gennaro, M., Cappelletti, P., Langella, A., Perrotta, A., Scarpati, C., 2000. Genesis of zeolites in the Neapolitan Yellow Tuff: geological, volcanological and mineralogical evidence. Contrib. Mineral. Petrol. 139, 17–35.

Dondi, M., Guarini, G., Venturi, I., 2001. Assessing the fusibility of feldspathic fluxes for ceramic tiles by hot stage microscope. Ind. Ceram. 21, 67–73.

Dondi, M., Cappelletti, P., D'Amore, M., de Gennaro, R., Graziano, S.F., Langella, A., Raimondo, M., Zanelli, C., 2016. Lightweight aggregates from waste materials: Reappraisal of expansion behavior and prediction schemes for bloating. Constr. Build. Mater. 127, 394–409. https://doi.org/10.1016/j.conbuildmat.2016.09.111.

El-Nile, A., Elazab, M., El-Zaiat, H., El-Azrak, K.E.-D., Elkomy, A., Sallam, S., Soltan, Y., 2021. In vitro and in vivo assessment of dietary supplementation of both natural or nano-zeolite in goat diets: Effects on ruminal fermentation and nutrients digestibility. Animals 11. https://doi.org/10.3390/ani11082215.

Eroglu, N., Emekci, M., Athanassiou, C.G., 2017. Applications of natural zeolites on agriculture and food production. J. Sci. Food Agric. https://doi.org/10.1002/jsfa.8312.

European Commission, 2023. European Critical Raw Materials Act - Establishing a Framework for Ensuring a Secure and Sustainable Supply of Critical Raw Materials and Amending Regulations (EU) 168/2013, (EU) 2018/858, 2018/1724 and (EU) 2019/1020.

Fantini, R., Argenziano, M., Cavalli, R., Arletti, R., Mino, L., 2024. Zeofilters for potentially innovative sunscreen products: formulation, stability and spectroscopic studies. J. Photochem. Photobiol. A Chem. 452 https://doi.org/10.1016/j.jphotochem.2024.115585.

Fedele, L., Scarpati, C., Lanphere, M., Melluso, L., Morra, V., Perrotta, A., Ricci, G., 2008. The Breccia Museo formation, Campi Flegrei, southern Italy: Geochronology, chemostratigraphy and relationship with the Campanian Ignimbrite eruption. Bull. Volcanol. 70, 1189–1219. https://doi.org/10.1007/s00445-008-0197-y.

Feoktistova, N., Akhmetova, V., Mukhitov, A., Ivanova, S., Ziruk, I., 2022. Silicon-Containing Minerals as Additives for Farm Animals, in: BIO Web of Conferences. https://doi.org/10.1051/bioconf/20225101003.

Fercia, M.L., Lonis, R., Peretti, R., Sau, A., Serci, A., Zucca, A., 2009. Mineralogical characteristics and cationic exchange properties of a zeolite mineral from Romana, NW Sardinia, Italy. Resour. Geol. 59, 15–24. https://doi.org/10.1111/j.1751-3928.2008.00077.x.

Fratini, N., 1949. Ricerche sulla calce di idrolisi nelle paste di cemento. Nota 1. Ann. Chim. Appl. 39, 41–49.

Fratini, N., 1950. Ricerche sulla calce di idrolisi nelle paste di cemento. Nota II. Proposta di saggio per la valutazione chimica dei cementi pozzolanici. Ann. Chim. Appl. 40, 461–469.

Fratini, C., Manganelli del Fa', C., Pecchioni, E., Scala, A., 1990. The sculptures in Bomarzo Park, Viterbo, Italy. In: Charola, A.E., Koestler, R.J., Lombardi, G. (Eds.), Proceedings of the International Meeting on Lavas and Volcanic Tuffs, Easter Island, pp. 129–141.

Gentili, S., Comodi, P., Nazzareni, S., Zucchini, A., 2014. The Orvieto-Bagnoregio Ignimbrite: Pyroxene crystal-chemistry and bulk phase composition of pyroclastic deposits, a tool to identify syn- and post-depositional processes. Eur. J. Mineral. 26, 743–756. https://doi.org/10.1127/ejm/2014/0026-2404.

Geological service - Tuscany region. Italy, 2013. Tuscany Geological Map 1:10.000 [WWW Document]. URL. http://www502.regione.toscana.it/geoscopio/cartoteca.html (accessed 9.6.23).

Ghoneem, W.M.A., El-Tanany, R.R., Mahmoud, A.E.M., 2022. Effect of natural zeolite as a Rumen buffer on growth performance and nitrogen utilization of Barki Lambs. Pak. J. Zool. 54, 1199–1207. https://doi.org/10.17582/journal.pjz/20191207121206.

Giampaolo, C., Mengarelli, L., Torracca, E., Spencer, C., 2008. Zeolite characterization of "Vico red tuff with black scoria" ignimbrite flow: the extractive district of Civita Castellana (Viterbo, Italy). Nuovo Cimento Soc. Ital. Fis., B 123, 1459–1476. https://doi.org/10.1393/ncb/i2008-10722-4.

Giordano, D., Russell, J.K., Dingwell, D.B., 2008. Viscosity of magmatic liquids: a model. Earth Planet. Sci. Lett. 271, 123–134. https://doi.org/10.1016/j.epsl.2008.03.038.

Girtan, M., Wittenberg, A., Grilli, M.L., de Oliveira, D.P.S., Giosuè, C., Ruello, M.L., 2021. The critical raw materials issue between scarcity, supply risk, and unique properties. Materials. https://doi.org/10.3390/ma14081826.

Graziano, S.F., Porzio, G., Di Benedetto, C., Dondi, M., Cappelletti, P., 2016. Expanded clays in water treatment: some alternative filtration media. Rend. Online Soc. Geol. Ital. 39, 159–162. https://doi.org/10.3301/ROL.2016.01.

Graziano, S.F., Zanelli, C., Molinari, C., de Gennaro, B., Giovinco, G., Correggia, C., Cappelletti, P., Dondi, M., 2022. Use of screen glass and polishing sludge in waste-based expanded aggregates for resource-saving lightweight concrete. J. Clean. Prod. 332 https://doi.org/10.1016/j.jclepro.2021.130089.

Gualtieri, A.F., Marchi, E., Passaglia, E., 1999. Zeolite content and cation exchange capacity of zeolite-rich rocks. Stud. Surf. Sci. Catal. 125, 707–713. https://doi.org/10.1016/S0167-2991(99)80277-8.

Her, S., Im, S., Liu, J., Suh, H., Kim, G., Sim, S., Wi, K., Park, D., Bae, S., 2024. Exploring the potential of pulverized oyster shell as a limestone substitute in limestone calcined clay cement (LC3) and its implications for performance. Constr. Build. Mater. 425 https://doi.org/10.1016/j.conbuildmat.2024.135918.

Herc, P., Bučko, O., Tirpák, F., Tokárová, K., Vizzarri, F., Massányi, P., Slanina, T., 2021. Effect of zeolite (Clinoptilolite) on chemical parameters of rabbit meat. J. Microbiol. Biotechnol. Food Sci. 11, 1–4. https://doi.org/10.15414/jmbfs.3986.

Holanda, D.M., Kim, Y.I., Parnsen, W., Kim, S.W., 2021. Phytobiotics with adsorbent to mitigate toxicity of multiple mycotoxins on health and growth of pigs. Toxins (Basel) 13. https://doi.org/10.3390/toxins13070442.

Holmes, D.A., 1994. Zeolites. In: Industrial Minerals and Rocks, 7th ed. Society for Mining, Metallurgy, and Exploration, Inc., Littleton CO, pp. 1129–1158.

Huntzinger, D.N., Eatmon, T.D., 2009. A life-cycle assessment of Portland cement manufacturing: comparing the traditional process with alternative technologies. J. Clean. Prod. 17, 668–675. https://doi.org/10.1016/j.jclepro.2008.04.007.

Ismail, U.M., Vohra, M.S., Onaizi, S.A., 2024. Adsorptive removal of heavy metals from aqueous solutions: progress of adsorbents development and their effectiveness. Environ. Res. 251 https://doi.org/10.1016/j.envres.2024.118562.

IUPAC ISO 15901-1-2005, 2005. Pore Size Distribution and Porosity of Solid Materials by Mercury Porosimetry and Gas Adsorption-Part 1: Mercury Porosimetry.

Izzo, F., Mercurio, M., de Gennaro, B., Aprea, P., Cappelletti, P., Daković, A., Germinario, C., Grifa, C., Smiljanic, D., Langella, A., 2019. Surface modified natural zeolites (SMNZs) as nanocomposite versatile materials for health and environment. Colloids Surf. B: Biointerfaces 182. https://doi.org/10.1016/j.colsurfb.2019.110380.

Izzo, F., Langella, A., de Gennaro, B., Germinario, C., Grifa, C., Rispoli, C., Mercurio, M., 2022. Chabazite from campanian ignimbrite tuff as a potential and sustainable remediation agent for the Removal of Emerging Contaminants from Water. Sustainability (Switzerland) 14. https://doi.org/10.3390/su14020725.

Jackson, M.D., Marra, F., Hay, R.L., Cawood, C., Winkler, E.M., 2005. The judicious selection and preservation of tuff and travertine building stone in ancient Rome. Archaeometry 47, 485–510. https://doi.org/10.1111/j.1475-4754.2005.00215.x.

Javed, T., Indu, I., Singhal, R.K., Shabbir, R., Shah, A.N., Kumar, P., Jinger, D., Dharmappa, P.M., Shad, M.A., Saha, D., Adamski, R., Siuta, D., 2022. Recent advances in agronomic and physio-molecular approaches for improving nitrogen use efficiency in crop plants. Front. Plant Sci. 13 https://doi.org/10.3389/fpls.2022.877544.

Jin, H.-Y., Yao, X.-Y., Tang, C.-C., Zhou, A.-J., Liu, W., Ren, Y.-X., Li, Z., Wang, A., He, Z.-W., 2024. Magnetite modified zeolite as an alternative additive to promote methane production from anaerobic digestion of waste activated sludge. Renew. Energy 224. https://doi.org/10.1016/j.renene.2024.120181.

Karge, H.G., 2001. Characterization by IR spectroscopy. In: Robson, H., Lillerud, K.P. (Eds.), Verified Syntheses of Zeolitic Materials, pp. 69–71.

Kaz'mina, O.V., 2010. Effect of the component composition and oxidation – reduction characteristics of mixes on foaming of pyroplastic silicate pastes. Glass Ceram. (English translation of Steklo i Keramika) 67, 109–113. https://doi.org/10.1007/s10717-010-9239-y.

König, R., Spaggiari, M., Santoliquido, O., Principi, P., Bianchi, G., Ortona, A., 2020. Micropollutant adsorption from water with engineered porous ceramic architectures produced by additive manufacturing and coated with natural zeolite. J. Clean. Prod. 258 https://doi.org/10.1016/j.jclepro.2020.120500.

Krajišnik, D., Daković, A., Milić, J., Marković, M., 2018. Zeolites as potential drug carriers. In: Modified Clay and Zeolite Nanocomposite Materials: Environmental and Pharmaceutical Applications, pp. 27–55. https://doi.org/10.1016/B978-0-12-814617-0.00002-5.

Kumar, N., Samota, S.R., Venkatesh, K., Tripathi, S.C., 2023. Global trends in use of nano-fertilizers for crop production: Advantages and constraints – a review. Soil Tillage Res. 228 https://doi.org/10.1016/j.still.2023.105645.

Landi, P., 1987. Stratigraphy and petrochemical evolution of Latera Volcano (Central Italy). Period. Mineral. 56, 201–224.

Langella, A., Bish, D.L., Cappelletti, P., Cerri, G., Colella, A., de Gennaro, R., Graziano, S. F., Perrotta, A., Scarpati, C., de Gennaro, M., 2013. New insights into the mineralogical facies distribution of Campanian Ignimbrite, a relevant Italian industrial material. Appl. Clay Sci. 72, 55–73. https://doi.org/10.1016/j.clay.2013.01.008.

Langella, A., Cappelletti, P., Mercurio, M., Calcaterra, D., de Gennaro, M., 2022. Building stones and technological materials of the Campi Flegrei Caldera, Italy, Active Volcanoes of the World. https://doi.org/10.1007/978-3-642-37060-1_14.

Langmuir, I., 1917. The constitution and fundamental properties of solids and liquids. J. Frankl. Inst. 183, 102–105. https://doi.org/10.1016/S0016-0032(17)90938-X.

Laurenzi, M.A., Villa, I., 1987. 40Ar/39Ar chronostratigraphy of Vico ignimbrites. Periodico di Mineralogia 56, 285–293.

Le Bas, M.J.L., Maitre, R.W.L., Streckeisen, A., Zanettin, B., 1986. A chemical classification of volcanic rocks based on the total alkali-silica diagram. J. Petrol. 27, 745–750. https://doi.org/10.1093/petrology/27.3.745.

Liguori, B., Iucolano, F., De Gennaro, B., Marroccoli, M., Caputo, D., 2015. Zeolitized tuff in environmental friendly production of cementitious material: chemical and mechanical characterization. Constr. Build. Mater. 99, 272–278. https://doi.org/10.1016/j.conbuildmat.2015.09.035.

Liguori, B., Aprea, P., Gennaro, B. de, Iucolano, F., Colella, A., Caputo, D., 2019. Pozzolanic activity of Zeolites: the Role of Si/Al Ratio. Materials 12, 4231. https://doi.org/10.3390/ma12244231.

Liu, X., Zhu, Z., 2024. Synthesis and catalytic applications of advanced Sn- and Zr-zeolites materials. Adv. Sci. 11 https://doi.org/10.1002/advs.202306533.

Liu, P., Wu, Q., Yan, K., Wang, L., Xiao, F.-S., 2024. Sustainable preparation of highly efficient copper ferroaluminosilicate CHA zeolite for selective catalytic reduction of NO_x with NH_3. J. Catal. 432 https://doi.org/10.1016/j.jcat.2024.115442.

Lo, T.Y., Tang, W.C., Cui, H.Z., 2007. The effects of aggregate properties on lightweight concrete. Build. Environ. 42, 3025–3029. https://doi.org/10.1016/j.buildenv.2005.06.031.

Mercurio, M., Izzo, F., Langella, A., Grifa, C., Germinario, C., Daković, A., Aprea, P., Pasquino, R., Cappelletti, P., Graziano, F.S., De Gennaro, B., 2018. Surface-modified phillipsite-rich tuff from the Campania region (southern Italy) as a promising drug carrier: an ibuprofen sodium salt trial. Am. Mineral. 103, 700–710. https://doi.org/10.2138/am-2018-6328.

Mercurio, M., Sarkar, B., Langella, A., 2019. Modified Clay and Zeolite Nanocomposite Materials Environmental and Pharmaceutical Applications. https://doi.org/10.1016/C2017-0-01250-8.

Miller, S.A., John, V.M., Pacca, S.A., Horvath, A., 2018. Carbon dioxide reduction potential in the global cement industry by 2050. Cem. Concr. Res. 114, 115–124. https://doi.org/10.1016/j.cemconres.2017.08.026.

Molinari, C., Zanelli, C., Guarini, G., Dondi, M., 2020. Bloating mechanism in lightweight aggregates: effect of processing variables and properties of the vitreous phase. Constr. Build. Mater. 261, 119980 https://doi.org/10.1016/j.conbuildmat.2020.119980.

Monteiro, M.A., Raupp-Pereira, F., Ferreira, V.M., Labrincha, J.A., Dondi, M., 2004. Lightweight aggregates made of industrial wastes or sub-products. In: Proc. RILEM 2004, Conference on the Recycled Materials in Building and Structures, 1, pp. 107–114.

Monteiro, M.A.A., Raupp-Pereira, F., Ferreira, V.M.M., Dondi, M., Labrincha, J.A.A., 2005. Lightweight aggregates based on industrial wastes. Ind. Ceram. 25, 157–163.

Montesano, G., Cappelletti, P., Caputo, D., Liguori, B., Campanile, A., Rispoli, C., 2022. Mineralogical and technological characterization of zeolites from basin and range as pozzolanic addition of cement. Materials 15. https://doi.org/10.3390/ma15072684.

Morante-Carballo, F., Montalván-Burbano, N., Carrión-Mero, P., Jácome-Francis, K., 2021. Worldwide research analysis on natural zeolites as environmental remediation materials. Sustainability (Switzerland) 13. https://doi.org/10.3390/su13116378.

Moreno Ríos, A.L., Gutierrez-Suarez, K., Carmona, Z., Ramos, C.G., Silva Oliveira, L.F., 2022. Pharmaceuticals as emerging pollutants: case naproxen an overview. Chemosphere. https://doi.org/10.1016/j.chemosphere.2021.132822.

Mormone, A., Ghiara, M.R., Balassone, G., Piochi, M., Lonis, R., Rossi, M., 2018. High-silica zeolites in pyroclastic flows from Central Sardinia (Italy): clues on genetic

processes and reserves from a mineralogical study. Mineral. Petrol. 112, 767–788. https://doi.org/10.1007/s00710-018-0583-x.
Mozgawa, W., Król, M., Barczyk, K., 2011. FT-IR studies of zeolites from different structural groups. CHEMIK nauka-technika-rynek 667–674.
Mueller, A., Sokolova, S.N.N., Vereshagin, V.I.I., 2008. Characteristics of lightweight aggregates from primary and recycled raw materials. Constr. Build. Mater. 22, 703–712. https://doi.org/10.1016/j.conbuildmat.2007.06.009.
Napolano, L., Menna, C., Graziano, S.F., Asprone, D., D'Amore, M., De Gennaro, R., Dondi, M., 2016. Environmental life cycle assessment of lightweight concrete to support recycled materials selection for sustainable design. Constr. Build. Mater. 119, 370–384. https://doi.org/10.1016/j.conbuildmat.2016.05.042.
Nappi, G., Renzulli, A., Santi, P., 1987. An evolutionary model for the Paleo-Bolsena and Bolsena Volcanic Complexes: a structural and petrographic study. Period. Mineral. 56, 241–267.
Nappi, G., Antonelli, F., Coltorti, M., Milani, L., Renzulli, A., Siena, F., 1998. Volcanological and petrological evolution of the Eastern Vulsini District, Central Italy. J. Volcanol. Geotherm. 87, 211–232.
Novembre, D., Gimeno, D., Cappelletti, P., Graziano, S.F., 2021. A case study of zeolitization process Tufo Rosso a Scorie Nere (Vico volcano, Italy): inferences for a general model. Eur. J. Mineral. 33, 315–328. https://doi.org/10.5194/ejm-33-315-2021.
Noviello, M., Gattullo, C.E., Faccia, M., Paradiso, V.M., Gambacorta, G., 2021. Application of natural and synthetic zeolites in the oenological field. Food Res. Int. 150 https://doi.org/10.1016/j.foodres.2021.110737.
Öz, M., 2024. Strategy to remove ammonium compounds released from fish feed in aquaculture using natural filtration materials. Environ. Monit. Assess. 196 https://doi.org/10.1007/s10661-024-12351-5.
Özen, S., Göncüoȟlu, M.C., Liguori, B., De Gennaro, B., Cappelletti, P., Gatta, G.D., Iucolano, F., Colella, C., 2016. A comprehensive evaluation of sedimentary zeolites from Turkey as pozzolanic addition of cement- and lime-based binders. Constr. Build. Mater. 105, 46–61. https://doi.org/10.1016/j.conbuildmat.2015.12.055.
Palladino, D.M., Simei, S., 2005. Eruptive dynamics and caldera collapse during the Onano eruption, Vulsini, Italy. Bull. Volcanol. 67, 423–440. https://doi.org/10.1007/s00445-004-0385-3.
Papaioannou, D., Katsoulos, P.D., Panousis, N., Karatzias, H., 2005. The role of natural and synthetic zeolites as feed additives on the prevention and/or the treatment of certain farm animal diseases: a review. Microporous Mesoporous Mater. 84, 161–170. https://doi.org/10.1016/j.micromeso.2005.05.030.
Pasquino, R., Di Domenico, M., Izzo, F., Gaudino, D., Vanzanella, V., Grizzuti, N., de Gennaro, B., 2016. Rheology-sensitive response of zeolite-supported anti-inflammatory drug systems. Colloids Surf. B: Biointerfaces 146, 938–944. https://doi.org/10.1016/j.colsurfb.2016.07.039.
Pavlak, M.S.D., Kaufmann, C., Eyng, C., Carvalho, P.L.O., Pozza, P.C., Vieites, F.M., Rohloff Junior, N., Avila, A.S., Polese, C., Nunes, R.V., 2023. Zeolite and corn with different compositions in broiler chickens feeding. Poult. Sci. 102 https://doi.org/10.1016/j.psj.2023.102494.
Peccerillo, A., 2017. Advances in Volcanology Cenozoic Volcanism in the Tyrrhenian Sea Region, Edition, 2nd ed. Springer Nature. https://doi.org/10.1007/978-3-319-42491-0.
Rashid, H., Rafey, A., 2023. Solid adsorbents for carbon dioxide capture: a review. Chem. Ecol. 39, 775–791. https://doi.org/10.1080/02757540.2023.2227622.
Renzulli, A., Santi, P., Balassone, G., Di Maio, G., De Bonis, A., Di Donato, V., Morra, V., 2018. Trachy-phonolite lava pebbles used in the ancient settlement of oplontis (Torre annunziata, Naples): petrochemical data supporting the origin from an old effusive activity of the somma-vesuvius volcano. Ann. Geophys. 61, 1–15. https://doi.org/10.4401/ag-7672.
Rolandi, G., De Natale, G., Kilburn, C.R.J., Troise, C., Somma, R., Di Lascio, M., Fedele, A., Rolandi, R., 2019a. The 39 ka campanian ignimbrite eruption: new data on source area in the campanian plain. In: Vesuvius, Campi Flegrei, and Campanian Volcanism. https://doi.org/10.1016/B978-0-12-816454-9.00008-0.
Rolandi, G., Di Lascio, M., Rolandi, R., 2019b. The neapolitan yellow tuff eruption as the source of the campi flegrei caldera. In: Vesuvius, Campi Flegrei, and Campanian Volcanism. https://doi.org/10.1016/B978-0-12-816454-9.00011-0.
Rouquerol, J., Baron, G., Denoyel, R., Giesche, H., Groen, J., Klobes, P., Levitz, P., Neimark, A.V., Rigby, S., Skudas, R., Sing, K., Thommes, M., Unger, K., 1994. Recommendations for the characterization of porous solids (Technical Report). Pure Appl. Chem. 66, 1739–1758. https://doi.org/10.1351/pac199466081739.
Selim, M.M., Tounsi, A., Gomaa, H., Shenashen, M., . Enhancing carbon capture efficiency in biogas upgrading: a comprehensive review on adsorbents and adsorption isotherms. AIP Adv. 14. https://doi.org/10.1063/5.0208686.
Serati-Nouri, H., Jafari, A., Roshangar, L., Dadashpour, M., Pilehvar-Soltanahmadi, Y., Zarghami, N., 2020. Biomedical applications of zeolite-based materials: a review. Mater. Sci. Eng. C. https://doi.org/10.1016/j.msec.2020.111225.
Serri, C., De Gennaro, B., Catalanotti, L., Cappelletti, P., Langella, A., Mercurio, M., Mayol, L., Biondi, M., 2016. Surfactant-modified phillipsite and chabazite as novel excipients for pharmaceutical applications? Microporous Mesoporous Mater. 224, 143–148. https://doi.org/10.1016/j.micromeso.2015.11.023.
Servatan, M., Zarrintaj, P., Mahmodi, G., Kim, S.J., Ganjali, M.R., Saeb, M.R., Mozafari, M., 2020. Zeolites in drug delivery: progress, challenges and opportunities. Drug Discov. Today. https://doi.org/10.1016/j.drudis.2020.02.005.
Shah, I.H., Miller, S.A., Jiang, D., Myers, R.J., 2022. Cement substitution with secondary materials can reduce annual global CO2 emissions by up to 1.3 gigatons. Nat. Commun. 13 https://doi.org/10.1038/s41467-022-33289-7.
Skhvitaridze, R., Giorgadze, I., Verulava, S., Shapakidze, E., Gejadze, I., Tsintskaladze, G., Kordzakhia, T., 2018. Scientific principles and practice in the use of natural mineral and industrial resources in the Georgian cement industry. Cement Int. 16, 70–77.
Smiljanić, D., de Gennaro, B., Izzo, F., Langella, A., Daković, A., Germinario, C., Rottinghaus, G.E., Spasojević, M., Mercurio, M., 2020. Removal of emerging contaminants from water by zeolite-rich composites: a first approach aiming at diclofenac and ketoprofen. Microporous Mesoporous Mater. 298 https://doi.org/10.1016/j.micromeso.2020.110057.
Smiljanić, D., de Gennaro, B., Daković, A., Galzerano, B., Germinario, C., Izzo, F., Rottinghaus, G.E., Langella, A., 2021. Removal of non-steroidal anti-inflammatory drugs from water by zeolite-rich composites: the interference of inorganic anions on the ibuprofen and naproxen adsorption. J. Environ. Manag. 286 https://doi.org/10.1016/j.jenvman.2021.112168.
Sparks, R.S.J., 1975. Stratigraphy and geology of the ignimbrites of Vulsini Volcano, Central Italy. Geol. Rundsch. 64, 497–523. https://doi.org/10.1007/BF01820680.
St. Cloud Mining Co, 2024. A Primary Producer of Natural Zeolite [WWW Document]. URL. http://www.stcloudmining.com/index.html.
Takarina, N.D., Matsue, N., Johan, E., Adiwibowo, A., Rahmawati, M.F.N.K., Pramudyawardhani, S.A., Wukirsari, T., 2024. Machine learning using random forest to model heavy metals removal efficiency using a zeolite-embedded sheet in water. Glob. J. Environ. Sci. Manag. 10, 321–336. https://doi.org/10.22034/gjesm.2024.01.20.
Taoufik, N., Boumya, W., Janani, F.Z., Elhalil, A., Mahjoubi, F.Z., Barka, N., 2020. Removal of emerging pharmaceutical pollutants: a systematic mapping study review. J. Environ. Chem. Eng. 8 https://doi.org/10.1016/j.jece.2020.104251.
Tokareva, A., Kaassamani, S., Waldmann, D., 2024. Using ceramic demolition wastes for CO2-reduced cement production. Constr. Build. Mater. 426 https://doi.org/10.1016/j.conbuildmat.2024.135980.
Turbeville, B.N., 1992. Vol a ~ 4~ Ages and Stratigraphy of the Latera caldera, Italy. Bull. Volcanol. 55, 110–118.
UNI EN 13055, 2016. Lightweight Aggregates.
UNI EN 196-5, 2015. Cement Test Methods - Part 5: Pozzolanic Test of Pozzolanic Cements.
Vafaee, F., Chaji, M., 2022. Use of acid-consuming bacteria and various buffers to improve digestion and fermentation of highly concentrated diets. Anim. Prod. Res. 11, 21–36. https://doi.org/10.22124/AR.2023.22294.1705.
Vahur, S., Teearu, A., Peets, P., Joosu, L., Leito, I., 2016. ATR-FT-IR spectral collection of conservation materials in the extended region of 4000-80 cm–1. Anal. Bioanal. Chem. 408, 3373–3379. https://doi.org/10.1007/s00216-016-9411-5.
Vaičiukynienė, D., Nizevičienė, D., Kantautas, A., Tamošaitis, G., Fornés, I.V., Krivenko, P., Boiko, O., 2024. Production of an eco-friendly concrete by including high-volume zeolitic supplementary cementitious materials and quicklime. Sci. Rep. 14 https://doi.org/10.1038/s41598-023-50761-6.
Valentine, G.A., Palladino, D.M., DiemKaye, K., Fletcher, C., 2019. Lithic-rich and lithic-poor ignimbrites and their basal deposits: Sovana and Sorano formations (Latera caldera, Italy). Bull. Volcanol. 81 https://doi.org/10.1007/s00445-019-1288-7.
Van Den Heede, P., De Belie, N., 2012. Environmental impact and life cycle assessment (LCA) of traditional and "green" concretes: Literature review and theoretical calculations. Cem. Concr. Compos. 34, 431–442. https://doi.org/10.1016/j.cemconcomp.2012.01.004.
Vereshchagin, V.I.I., Sokolova, S.N.N., 2006. Formation of a porous structure in a granulated glass ceramic material from zeolite-bearing rock with alkali additives. Glass Ceram. (English translation of Steklo i Keramika) 63, 227–229. https://doi.org/10.1007/s10717-006-0085-x.
Vezzoli, L., Conticelli, S., Innocenti, F., Landi, P., Manetti, P., Palladino, D.M., Trigila, R., 1987. Stratigraphy of the Latera Volcanic complex: proposal for a new nomenclature. Genesis and evolution of TMVB View project Lamprophyric magmatism in the NW Iran View project. Period. Mineral. 56, 89–110.
Volland, S., Brötz, J., 2015. Lightweight aggregates produced from sand sludge and zeolitic rocks. Constr. Build. Mater. 85, 22–29. https://doi.org/10.1016/j.conbuildmat.2015.03.018.
Wang, H., Yin, J., Kim, I.H., 2021. Experimental study on the effect of zeolite (clinoptilolite) on the growth performance, nutrient digestibility, and faecal microbiota of finishing pigs. J. Appl. Anim. Res. 49, 154–157. https://doi.org/10.1080/09712119.2021.1914063.
Washington, H.S., 1906. The Roman Comagmatic Region. Carnegie Instiution of Washington, Washington, D. C.
Wei, L., Yao, Z., Li, H., Guo, H., Li, Y., 2024. Mechanical Properties of Aeolian Sand Concrete made from Alkali-Treated Aeolian Sand and Zeolite Powder. Materials 17. https://doi.org/10.3390/ma17071537.
Yudi, A., Nabila, S., Naghazta, M.G., Rindu Trisna, W., 2024. Utilization of Zeolite Materials with Physical Activation and Chemical Activation as Cement Substitutes, in: AIP Conference Proceedings. https://doi.org/10.1063/5.0205079.
Zhou, P., Wang, F., Shen, Y., Duan, X., Zhao, S., Chen, X., Liang, J., 2024. Removal of emerging organic pollutants by zeolite mineral (clinoptilolite) composite photocatalysts in drinking water and watershed water. Catalysts 14. https://doi.org/10.3390/catal14040216.
Zhu, H., Wu, X., Zhang, Y., Li, H., 2024. Fast setting and high early strength alkali-activated fly ash synthetized with pre-polymerized suspension combined with ultrafine fly ash at ambient temperature. Case Stud. Construct. Mater. 20 https://doi.org/10.1016/j.cscm.2024.e02939.